Received: 19 November 2016 | Accepted: 11 July 2017

DOI: 10.1111/2041-210X.12904

RESEARCH ARTICLE

Methods in Ecology and Evolution | BRITISH ECOLOGICAL SOCIETY

Estimation of above-ground biomass of large tropical trees with terrestrial LiDAR

Jose Gonzalez de Tanago[1,2] | Alvaro Lau[1,2] | Harm Bartholomeus[1] | Martin Herold[1] | Valerio Avitabile[1] | Pasi Raumonen[3] | Christopher Martius[2] | Rosa C. Goodman[4] | Mathias Disney[5,6] | Solichin Manuri[7] | Andrew Burt[5] | Kim Calders[5,8]

[1]Laboratory of Geo-Information Science and Remote Sensing, Wageningen University & Research, Wageningen, The Netherlands; [2]Center for International Forestry Research (CIFOR), Bogor, Indonesia; [3]Laboratory of Mathematics, Tampere University of Technology, Tampere, Finland; [4]Department of Forest Ecology and Management, Swedish University of Agricultural Sciences (SLU), Umeå, Sweden; [5]Department of Geography, University College London, London, UK; [6]NERC National Centre for Earth Observation (NCEO), Leicester, UK; [7]Fenner School of Environment and Society, Australian National University, Canberra, ACT, Australia and [8]Earth Observation, Climate and Optical group, National Physical Laboratory, Teddington, UK

Correspondence
Jose Gonzalez de Tanago
Email: jose.tanago@gmail.com

Funding information
Norwegian Agency for Development Cooperation (Norad); Australian Department of Foreign Affairs and Trade (DFAT); European Union; International Climate Initiative (IKI) of the German Federal Ministry for the Environment, Nature Conservation, Building and Nuclear Safety (BMUB); CGIAR Fund; SilvaCarbon, Grant/Award Number: 14-IG-11132762-350; UK NERC National Centre for Earth Observation (NCEO)

Handling Editor: Darren Kriticos

Abstract

1. Tropical forest biomass is a crucial component of global carbon emission estimations. However, calibration and validation of such estimates require accurate and effective methods to estimate in situ above-ground biomass (AGB). Present methods rely on allometric models that are highly uncertain for large tropical trees. Terrestrial laser scanning (TLS) tree modelling has demonstrated to be more accurate than these models to infer forest AGB. Nevertheless, applying TLS methods on tropical large trees is still challenging. We propose a method to estimate AGB of large tropical trees by three-dimensional (3D) tree modelling of TLS point clouds.
2. Twenty-nine plots were scanned with a TLS in three study sites (Peru, Indonesia and Guyana). We identified the largest tree per plot (mean diameter at breast height of 73.5 cm), extracted its point cloud and calculated its volume by 3D modelling its structure using quantitative structure models (QSM) and converted to AGB using species-specific wood density. We also estimated AGB using pantropical and local allometric models. To assess the accuracy of our and allometric methods, we harvest the trees and took destructive measurements.
3. AGB estimates by the TLS–QSM method showed the best agreement in comparison to destructive harvest measurements (28.37% coefficient of variation of root mean square error [CV-RMSE] and concordance correlation coefficient [CCC] of 0.95), outperforming the pantropical allometric models tested (35.6%–54.95% CV-RMSE and CCC of 0.89–0.73). TLS–QSM showed also the lowest bias (overall underestimation of 3.7%) and stability across tree size range, contrasting with the allometric models that showed a systematic bias (overall underestimation ranging 15.2%–35.7%) increasing linearly with tree

This is an open access article under the terms of the Creative Commons Attribution License, which permits use, distribution and reproduction in any medium, provided the original work is properly cited.
© 2017 The Authors. *Methods in Ecology and Evolution* published by John Wiley & Sons Ltd on behalf of British Ecological Society.

size. The TLS–QSM method also provided accurate tree wood volume estimates (CV RMSE of 23.7%) with no systematic bias regardless the tree structural characteristics.

4. Our TLS–QSM method accounts for individual tree biophysical structure more effectively than allometric models, providing more accurate and less biased AGB estimates for large tropical trees, independently of their morphology. This non-destructive method can be further used for testing and calibrating new allometric models, reducing the current under-representation of large trees in and enhancing present and past estimates of forest biomass and carbon emissions from tropical forests.

KEYWORDS

above-ground biomass, allometric models, LiDAR, terrestrial laser scanning, tree volume, tropical trees, 3D modeling

1 | INTRODUCTION

The above-ground carbon in tropical forests represents 40% of the total carbon stocked in forests globally (Gibbs, Brown, Niles, & Foley, 2007). However, the estimation of tropical forest carbon stocks presents large uncertainties (Mitchard et al., 2013, 2014). Forest carbon stocks are not measured directly, but derived either from interpolation or extrapolation of point estimates of the above-ground biomass (AGB) contained in forest inventory plots, or from measurements of remote sensing proxies calibrated with plot-based AGB estimates (Gibbs et al., 2007).

The only way to truly and directly measure forest AGB implies cutting and weighing the mass of all trees in the plot, which is costly and causes a negative impact, and is thus seldom executed (Clark & Kellner, 2012). Instead, plot AGB is estimated from aggregation of individual tree AGB estimates. These tree AGB estimates are indirectly derived from easily measured tree parameters (diameter at breast height [DBH], height and wood density derived from tree species identification) by means of allometric models, which relate these tree parameters with real tree AGB measured in destructive sampling studies (Chave et al., 2005). This indirect estimation approach introduces an error propagation chain. The biggest source of error is derived from the allometric models, hence its appropriate selection is the most important aspect to improve the accuracy of AGB estimates (Molto, Rossi, & Blanc, 2013).

The uncertainty in the tree AGB estimation is even greater for large tropical trees (DBH >70 cm) because AGB in large trees varies more than in small trees (Chave et al., 2005; Goodman, Phillips, & Baker, 2014; Ploton et al., 2016; Slik et al., 2013), and due to the presence of buttresses is prone to larger measurement error (Chave et al., 2014). Moreover, it is particularly relevant to accurately estimate AGB of large trees because of their major influence on the tropical forest AGB variation (Slik et al., 2013; Stegen et al., 2011).

As an alternative, remote sensing systems can be used to estimate tropical forest carbon stocks. One of the most promising remote sensing approaches to estimate forest AGB is via light detection and ranging (LiDAR), either via spaceborne platforms (e.g. ICESat), airborne laser scanning or terrestrial laser scanning (TLS). Laser pulses from LiDAR instruments can penetrate the forest canopy providing good estimates of forest canopy heights and structure, from which AGB along the vertical profile and canopy cover can be estimated (Goetz & Dubayah, 2011).

TLS data provide the highest level of three-dimensional (3D) detail of forest and tree structure (Newnham et al., 2015). Currently, TLS data are being used to model 3D structure of individual trees allowing direct measurements of forest and tree structural parameters such as DBH (Bauwens, Bartholomeus, Calders, & Lejeune, 2016), tree height (Király & Brolly, 2007), crown dimensions (Holopainen, Vastaranta, & Kankare, 2011) and individual branches (Raumonen, Kaasalainen, Kaasalainen, & Kaartinen, 2011). Several review articles provide additional information about the characteristics of TLS and its use for forestry surveying (Newnham et al., 2015).

Several approaches estimate forest AGB by exploiting the capability of TLS data to characterize forest structure at tree level. A simple approach is to measure tree structural parameters from a TLS 3D point cloud and apply allometric models to relate the measured parameters with AGB (e.g. Yao et al. (2011)). However, this method still relies on allometric models. A different kind of approach has been developed to reconstruct the complete 3D tree architecture from TLS data rather than a single or few structural parameters. Quantitative structure models (QSMs; Delagrange, Jauvin, & Rochon, 2014; Hackenberg, Wassenberg, Spiecker, & Sun, 2015; Raumonen et al., 2013) are architectural tree models reconstructed from the TLS point cloud of individual trees and allow volume measurements. The estimated tree volume is converted to tree AGB by multiplying it by the specific wood density (Calders, Newnham, et al., 2015; Hackenberg et al., 2015). Thus, this method estimates AGB based on the biophysical modelling of specific tree structure rather than the allometric models which are based on empirical relationships from a sample of trees and rely on a limited number of tree structural parameters.

The QSM reconstruction method developed by Raumonen et al. (2013) has been applied for wood volume estimation and AGB

estimation in boreal and temperate forest (Raumonen et al., 2015) and in more structurally complex tropical forests in Gabon (Disney et al., 2014). AGB estimates derived from this approach in Australia showed a higher agreement with reference values from destructive sampling (coefficient of variation of root mean square error [CV RMSE] = 16.1%) compared to AGB estimates derived by allometric models (CV RMSE = 46.2%–57%) (Calders, Newnham, et al., 2015). However, the accuracy of AGB estimates in tropical forest trees has not been investigated yet with reference data.

Several challenges arise when one wants to estimate tree AGB in a tropical forest using QSM. First, for very large and complex trees there is a lack of reference data to validate the 3D reconstruction models from TLS. Furthermore, the structural complexity of a tropical forest can potentially have a large influence on acquired TLS data. This requires careful design of an appropriate scanning pattern to diminish vegetation occlusion and to allow accurate reconstruction of the 3D structure of trees (Wilkes et al., 2016).

Here, we assess the potential and accuracy of volume reconstruction using QSMs for estimating AGB of large tropical forest trees. For this, 29 plots were scanned with TLS and one large tree per plot was destructively sampled afterwards. With the TLS data acquired, we (1) optimized the QSM tree volume reconstruction method based on a subsample of nine of the 29 trees. After each tree was scanned and harvested, we (2) performed in situ destructive measurements to independently estimate tree volume for comparison with model estimates and calculate their accuracy. Finally, using the independent tree dataset (remaining 20 trees non-used in point 1), we (3) compared the accuracy of the AGB estimates based on QSMs with the accuracy of the AGB estimates based on pantropical and local allometric models.

2 | MATERIALS AND METHODS

2.1 | Study area

We acquired field data from 29 plots across three tropical forest sites in Peru, Indonesia and Guyana. Table 1 shows the description of each site.

2.2 | TLS sampling and field data collection

Plots were established around a tree to be harvested after the laser scanning. Plot spatial design and tree selection are detailed in Appendix S1. Once the plots were set up, we scanned the plot with TLS, performed a forest inventory, harvested the selected tree and measured the geometric structure of the harvested tree.

2.2.1 | TLS data acquisition

TLS datasets were acquired using a RIEGL VZ-400 3D® terrestrial laser scanner (RIEGL Laser Measurement Systems GmbH, Horn, Austria). This scanner is a discretized multiple-return LiDAR scanner and its specifications are shown in Table 2. Details of the sampling design are described in Appendix S2.

2.2.2 | Forest inventory data collection

For each tree, we measured DBH (or diameter above buttresses), tree height, height of first branch and crown width. We measured DBH with a forestry tape and tree height with a Nikon "Forestry-Pro" (Hayama, Japan) laser hypsometer with precisions of 0.01 and 0.2 m respectively. An experienced taxonomist (specialist of the local flora) identified the trees at species level.

2.2.3 | Harvested tree reference measurements

We measured the geometry of the stem, buttresses and branches of each harvested tree. As in Figure 1(1), tree stem diameters (1a) were

TABLE 2 Terrestrial laser scanning specifications

Wavelength	1,550 nm
Beam divergence	0.35 mrad
Scan range	360° in azimuth 100° in zenith
Scan resolution	0.06°

TABLE 1 Study sites description

	Peruvian site	Indonesian site	Guyanese site
Number of plots	9	10	10
Forest type	Lowland tropical moist *terra firme* forest	Peat swamp forest	Lowland tropical moist forest
Region	Madre de Dios. South western Amazon	Mentaya River (Central Kalimantan)	Vaitarna Holding's concession
Lat/long	−12.27 lat −69.10 long	−2.41 lat 113.13 long	6.04 lat −58.70 long
Mean elevation	312 m a.s.l.	22 m a.s.l.	117 m a.s.l.
Mean yearly rainfall[a]	2,074 mm	2,616 mm	2,195 mm
Mean stem density (trees with diameter at breast height [DBH] > 10 cm)	565 stems/ha	1,314 stems/ha	516 stems/ha
Mean DBH harvested trees (*SD*)	90.0 cm (22.2 cm)	58.4 cm (18.2 cm)	73.7 cm (12.0 cm)

[a]From Muñoz & Grieser (Muñoz & Grieser, 2006).

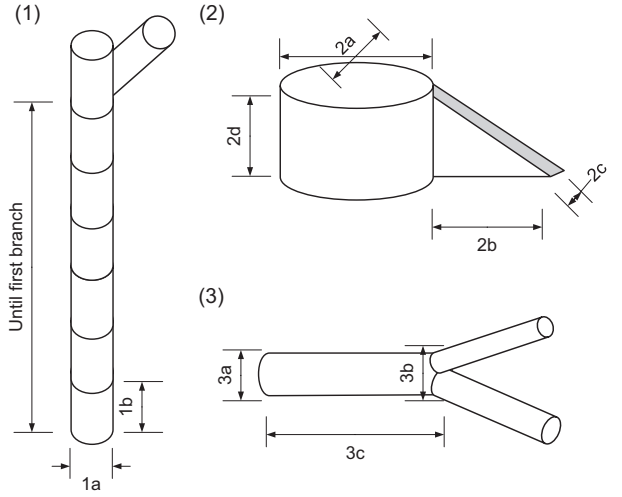

FIGURE 1 Tree geometry measurements. (1) Stem diameter (1a) every metre (1b) until start of first branch. For trees with buttresses (2): diameter in two orthogonal directions (2a) and for each buttress horizontal length (from the furthest point to the stem) (2b); width (mean width between the tip and the buttress intersection with the stem) (2c); and height (from the ground to the highest insertion point of the buttress into the stem) (2d). For branches (3): proximal diameter at the base of each internode and above flaring (3a), distal diameter at the tip of each internode and below flaring of the next node (3b) and branch length from the base to the tip of each internode (3c)

measured at every metre along the stem (1b) following the approach of Kankare et al. (2013). For trees with buttresses or major irregularities, we measured as in Figure 1(2). Finally, we measured all branches until tapered diameter ≤10 cm by measuring each internode independently as in Figure 1(3).

2.3 | Volume and biomass estimation

2.3.1 | Tree wood volume estimation from 3D QSM

We co-registered each individual TLS scan into a single plot point cloud using RiScan Pro software (version 2.0; RIEGL Laser Measurement Systems GmbH, www.riegl.com) and the accuracy of our co-registration was kept below 1 cm.

We reconstructed the woody structure of trees using the QSM method developed by Raumonen et al. (2013) and further developed by Calders, Newnham, et al. (2015) and Raumonen et al. (2015). The method first segments the TLS point cloud reconstructing the whole tree topological branching architecture and then reconstructs the surface and volume of the segments by fitting cylinders to each of the segments (Figure 2). The resulting cylinder models are used for automatic calculation of the volume of the whole woody fraction of individual trees (trunk and branches). More details are provided in Appendix S3.

We filtered out cylinders with diameter <10 cm from resulting QSMs to be consistent with the reference volume estimation and we calculated the total tree volume by summing the volume of all remaining cylinders. Due to the random generation of the QSM patches (point cloud partition into small segments) (Calders, Newnham, et al., 2015; Raumonen et al., 2015), for each parameter set used we reconstructed 20 QSMs and averaged the volume of the 20 model realizations.

2.3.2 | Sensitivity analysis and independent estimation of QSM accuracy

We split our tree population into two independent sub-datasets using stratified random sampling without replacement: a tree dataset of nine trees (three from each study area) for the sensitivity analysis of a QSM parameter value, and a second tree dataset of 20 trees (the remaining six trees for Peru and seven for Guyana and Indonesia) for independent estimation of tree volume and AGB estimates accuracy.

The reconstruction of the QSMs requires a few input parameters, of which the size of the point cloud segments—expressed by the "surface patches diameter" (hereafter "*PatchDiam*")—had the most influence on the outcome (Calders, Newnham, et al., 2015). A detailed explanation of the QSM parameters and QSM sensitivity to them is provided in the Supporting Information and in Raumonen et al. (2013, 2015) and Calders, Newnham, et al. (2015).

Our sensitivity analysis consisted of the evaluation of the QSMs optimal *PatchDiam* value, which gives the most accurate volume estimate among the different *PatchDiam* values tested (1, 2.5, 5, 7.5, 10 and 15 cm). For each tree in the sensitivity analysis tree dataset, we compared the mean estimated volume (from the 20 QSM realizations per *PatchDiam*) against the tree volume obtained from the destructive measurements. We computed tree volume estimation RMSE. The optimal *PatchDiam* was chosen as the one that minimized the RMSE.

Once the optimal *PatchDiam* was found, we assessed the stability of the optimization procedure. We replicated the stratified

FIGURE 2 Example of one tree terrestrial laser scanning point cloud from Guyana dataset (left, in dark red), and the same tree modelled by quantitative structure models (right, in green). Figure from Gonzalez de Tanago et al. (2016)

random sampling 1,000 times and analysed the frequency of optimal *PatchDiam*'s obtained (the one providing the smallest RMSE in each of the 1,000 samples) as well as the variability of the RMSE results (range, mean and standard deviation) for all samples with a given optimal *PatchDiam*.

Finally, the optimized *PatchDiam* was used to run QSM for the independent estimation dataset (20 trees) and to calculate the tree volume following the same procedure described above. We used MATLAB (The MathWorks Inc. 2014) for QSM reconstruction and "R" (R Core Team 2013) for further calculations.

2.3.3 | Tree volume estimation from reference measurements

We used the reference geometric measurements (Section 2.2.3) from each harvested tree to determine the tree reference volume. We applied the Smalian formula as in Nogueira, Nelson, and Fearnside (2005) to estimate volume of stem sections and individual branches until 10 cm diameter, while for the buttresses we applied a general prism volume formula. Detailed information can be found in Appendix S4. Total tree wood volume was calculated as the sum of volumes of main stem, large branches (>10 cm diameter) and buttresses.

As in Berger, Gschwantner, McRoberts, and Schadauer (2014), any misrepresentation of the main stem and branches volumes by the Smalian approximation and any measurement error taken were considered negligible and ignored. Furthermore, the sum of all cylinders was assumed to represent the true tree volume with no error and that the wood volume was measured without error.

2.3.4 | Tree AGB estimation from volume models and wood density

We calculated individual tree AGB by multiplying individual tree wood volume estimates by the specific basic wood density (ρ). Values of ρ were assigned to the finest taxonomic level possible (species, genus or family) according to the Global Wood Density Database (Chave et al., 2009; Zanne et al., 2009) and tree species identified in the field. We applied an expansion factor accounting for small branches (≤10 cm diameter). The expansion factor related the volume of small branches to the one of the large branches (>10 cm diameter). We calculated an expansion factor of 0.255 using data from biomass destructive sampling of 51 trees in a nearby Peruvian Amazon forest site (Goodman, Phillips, & Baker, 2013; Goodman et al., 2014). We used the same value for Peru and Guyana (0.255), while we calculated the expansion factor for Indonesia (0.28) from our own collected data. The final contribution of small branches to tree volume was 10%, 14% and 7% for Guyana, Peru and Indonesia respectively.

2.3.5 | Tree AGB estimation from allometric models

We estimated AGB using 12 allometric models, of which eight were locally calibrated and four pantropical (see Appendix S5). The pantropical allometric models used were developed by Chave et al. (2005), which have been recently improved (Chave et al., 2014).

The local allometric models used for the Peruvian trees were developed by Goodman et al. (2014), while allometric models for Indonesian trees were developed by Manuri et al. (2014) and Jaya, Siregar, Daryono, and Suhartana (2007). No suitable local allometric model could be found for Guyana. The details of the allometric models used to estimate AGB for the harvested trees are described in the Supporting Information.

2.4 | AGB estimation models accuracies and uncertainty assessment

We used the 20 trees in the dataset reserved for the independent estimation to compare the accuracy of AGB estimates from our TLS–QSM approach (against reference AGB) vs. the accuracy obtained from allometric models (against reference AGB). The model error was calculated for each tree and for the mean of the 20 trees using several metrics. The AGB estimation error (residual, in Mg) (Equation 1) and individual tree relative error (in %) (Equation 2) were calculated for each tree, while model bias (in %) (Equation 3) was calculated as the mean of the estimation errors divided by the mean of reference AGB.

$$\mathrm{AGB}_{\text{estimation errors}}(\mathrm{Mg}) = \mathrm{AGB}_{\text{model}} - \mathrm{AGB}_{\text{ref}} \tag{1}$$

$$E_{\text{relative}}(\%) = \left(\frac{\mathrm{AGB}_{\text{model}} - \mathrm{AGB}_{\text{ref}}}{\mathrm{AGB}_{\text{ref}}}\right) \times 100 \tag{2}$$

$$\mathrm{Model}_{\text{bias}}(\%) = \left(\frac{\sum_1^n \mathrm{AGB}_{\text{estimation errors}} \div n}{\text{Mean AGB}_{\text{ref}}}\right) \times 100 \tag{3}$$

where $\mathrm{AGB}_{\text{model}}$ is the AGB estimated by the model and $\mathrm{AGB}_{\text{ref}}$ is the AGB observed (AGB calculated from destructive measurements).

As general indicators of model accuracy, RMSE (in m^3 and Mg), CV RMSE (in %) and mean relative error (in %) were calculated. Slope and intercept values of orthogonal regression models between AGB modelled and reference values were used to identify departure from the 1:1 line, and the R-squared (hereafter R^2) was used to judge the fitting of these regressions. Finally, the concordance correlation coefficient (CCC) was calculated to compare agreement of AGB model estimates with AGB reference and to previously reported agreement using the QSM method (Calders, Newnham, et al., 2015).

To assess the uncertainty in the tree AGB estimations, we used the error propagation approach (Equation 4) to account for the uncertainties in the models components. We combined them and assumed that the uncertainties were statistically independent (not correlated and with a Gaussian distribution). We used Equation 4 expressing model uncertainties in percentage terms:

$$U_{\text{total}} = \sqrt{U_1^2 + U_2^2} \tag{4}$$

where U_{total} is the propagated uncertainty (as percentage) from the model components, U_1 and U_2 are the uncertainties (as percentage) from each component (IPCC 2006).

For AGB estimations from QSM volume models, the model uncertainty components considered were the wood volume and wood density. The uncertainty in tree wood volume by QSM is provided by the standard deviation of the 20 QSM realizations per tree. For the estimation of wood densities uncertainties, we assumed for all species the same standard deviation of 10% of the mean as used by Chave et al. (2004). Likewise, to assess the uncertainty in the tree AGB estimation from allometric models, we used the uncertainties reported for each model (see Appendix S5). To assess the uncertainty in the tree AGB estimation from reference volume estimates, we considered two components: wood density (as described for QSM) and expansion factor. For the expansion factor, we assumed an error of 12.5% as reported in Segura and Kanninen (2005).

3 | RESULTS

3.1 | Tree volume estimation with QSM

The results of the tree volume modelling with the TLS–QSM approach are divided into two steps: (1) QSM sensitivity analysis with nine trees to determine QSM optimal parameters and then (2) an independent assessment of the tree volume estimation accuracy with an independent sample of 20 trees.

3.1.1 | Sensitivity analysis of QSM tree volume modelling

The TLS–QSM tree volume estimation error (RMSE) when compared with the reference volume measurements decreased with decreasing *PatchDiam* (Table 3) until it reached a minimum error for *PatchDiam* of 2.5 cm, and then it increased again for smaller *PatchDiam*. This is in line with the results of the sensitivity analysis in Calders, Burt, et al. (2015) and Calders, Newnham, et al. (2015). Therefore, 2.5 cm was considered the optimal *PatchDiam*, and thus selected for the tree volume estimation of the remaining tree dataset.

The stability assessment of *PatchDiam* optimization procedure showed that in 75% of the 1,000 random sampling replicates the optimal *PatchDiam* was 2.5 cm. Despite the relatively small sample reserved for the sensitivity analysis (9 out of 29 trees), the optimal *PatchDiam* was relatively stable regardless of the characteristics of the randomly selected trees.

TABLE 3 QSM volume sensitivity analysis

PatchDiam (cm)	RMSE (m^3)	CV RMSE (%)	Mean relative error (%)
1.0	3.42	27.56	10.31
2.5	2.98	23.92	17.67
5.0	4.60	36.97	31.87
7.5	7.11	57.17	49.42
10.0	9.06	72.81	65.07
15.0	13.32	107.09	98.05

PatchDiam, surface patches diameter; QSM, quantitative structure models; CV RMSE, coefficient of variation of root mean square error.

3.1.2 | Independent assessment of tree volume estimation from TLS–QSM

To assess the accuracy of the tree wood volume estimation by the TLS–QSM, we compared the volume estimates by the TLS–QSM with the reference volume estimates from destructive measurements (Figure 3).

The R^2 of the linear model describing the agreement of both datasets (Figure 3 blue line) was 0.9. Its slope was 0.93 indicating that the QSMs slightly underestimated the tree volume for the largest trees. The RMSE was 3.29 m^3, compared with the mean tree volume of 15.13 m^3, leading to a CV RMSE of 23.7%. Figure 3 shows that the TLS–QSM performed similarly throughout the three different sites, despite the three study areas contained different tree species, sizes and shapes. Results differ between "small trees" (DBH ≤ 70 cm, corresponding approximately with 9 Mg, hereafter *small trees*) and "large trees" (DBH > 70 cm, hereafter *large trees*). For *small trees*—which were mostly part of the Indonesian dataset—TLS–QSM models showed less uncertainty and less deviation from the reference compared to *large trees*.

On the other hand, the analysis of the residuals (Figure 4) reveals that for *small trees* and *large trees* the model did not systematically tend to overestimate nor underestimate the volume. Despite the larger uncertainty in the volume estimation for *large trees*, there was no large systematic bias for larger tree size (Figure 4).

Buttresses were predominately absent in *small trees*, which had a better agreement with the reference data than trees with buttresses.

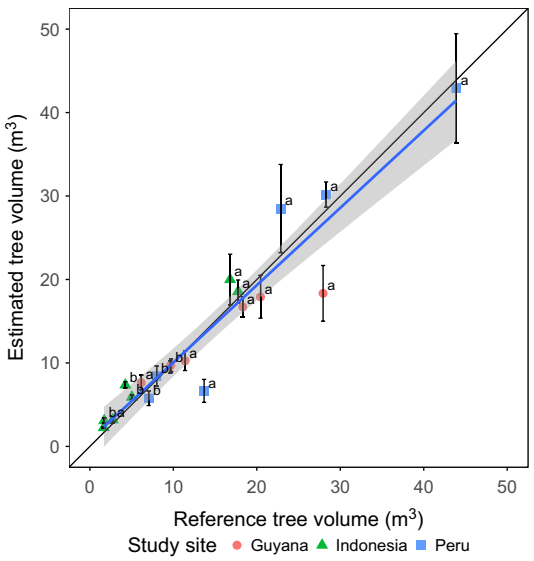

FIGURE 3 Scatterplot of tree volume estimation by terrestrial laser scanning–quantitative structure models (QSM; *y*-axis) against reference measurements (*x*-axis). The solid black line depicts the 1:1 line. Error bars are the standard deviation of the 20 QSM model realizations per tree. Symbols and colours denote values per study site. The blue line depicts the fitted linear regression model between QSM volume estimates and reference volume estimates, and grey bands show the 95% confidence interval of this regression. Coefficient "a" denotes tree with buttresses and "b" tree with no buttresses

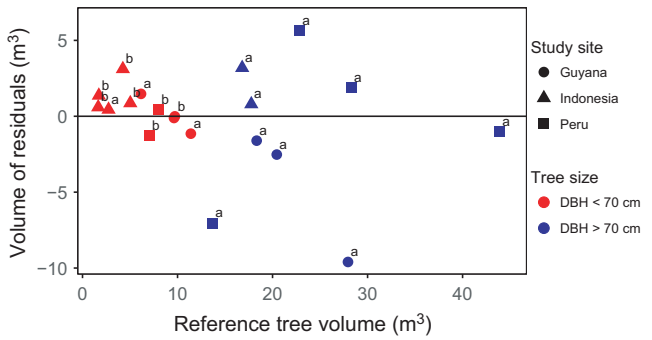

FIGURE 4 Analysis of volume estimation residuals. Trees with diameter at breast height (DBH) ≤ 70 cm were classified as small size trees (red colour) and trees with DBH > 70 cm were classified as large trees (blue colour). Coefficient "a" denotes tree with buttresses while coefficient "b" denotes absence of tree buttresses

Our QSM modelling did not perform a detailed buttress modelling, but a cylinder fitting, which might be the cause of the higher residuals in the trees with buttresses.

3.2 | Comparison of AGB estimation accuracies: TLS–QSM vs. allometric models

3.2.1 | Overall accuracy across study sites: TLS–QSM vs. pantropical allometric models

Figure 5 shows the agreement between the AGB estimates by TLS–QSM and allometric models (*modelled*) and derived from the destructive measurements (*reference*) for the independent assessment tree dataset. The high level of agreement with the *AGB-reference* provided by the TLS–QSM approach (CCC = 0.95) contrasts with the systematic AGB underestimation of the allometric models for *large trees* (CCC = 0.73–0.89).

Table 4 shows the statistical indicators of the accuracy of AGB estimations based on the TLS–QSM approach and pantropical allometric models for the mean of the 20 trees in the independent assessment dataset.

The TLS–QSM method had the lowest RMSE, which was 20% and almost 50% lower than the most accurate (Chave05.m.1.3) and the least accurate allometric model (Chave14.eq.4) respectively. The TLS–QSM approach also had the lowest bias, 75% and 90% lower than the most and the least accurate allometric models respectively. The TLS–QSM AGB estimates also showed the most consistent agreement with the reference AGB (CCC = 0.95) along the range of AGB reference values with no major systematic deviation to the 1:1 line (slope of 1.06), whereas the best allometric model (slope of 0.77) showed a systematic increasing underestimation of AGB for *large trees* and a lower agreement with reference AGB (CCC = 0.89). The trend of systematic increasing underestimation of AGB for larger trees was even more pronounced for less accurate allometric models (slopes ranging from 0.66 to 0.60) showing a lower agreement compared to reference AGB (CCC = 0.73–0.82).

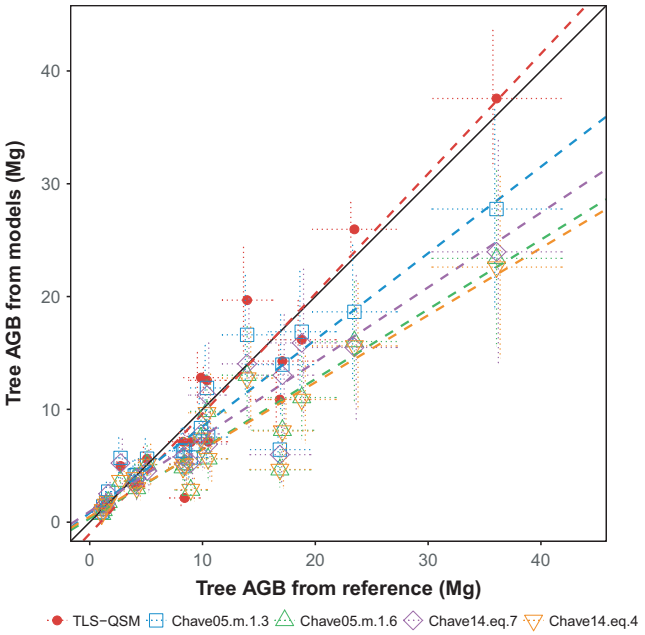

FIGURE 5 Scatterplot of above-ground biomass (AGB) estimates by terrestrial laser scanning–quantitative structure models (TLS–QSM) approach and pantropical allometric models (*y*-axis) against the AGB reference values (*x*-axis). The 1:1 line is depicted as a black solid line. The dashed lines represent the fitted orthogonal models between AGB estimates by TLS–QSM or pantropical allometric models and AGB reference, with colours corresponding the colour used for the model estimates. Vertical bars show the estimated uncertainty (standard deviation) for each model estimate and horizontal bars show the uncertainty for the reference AGB estimates

3.2.2 | Overall accuracy within study sites: TLS–QSM vs. local allometric models

Figure 6 displays the agreement between the *AGB-modelled* based on the TLS–QSM approach and local allometric models (*y*-axis) against *AGB-reference* (*x*-axis) for the sites where local allometric models were available.

For the Peruvian study area the TLS–QSM approach is the closest to the 1:1 line, whereas the deviation from the 1:1 line is clearly larger for the three local allometric models tested, which systematically underestimate the AGB of *large trees*. The TLS–QSM approach showed 10% and 50% lower RMSE and 80% and 85% lower bias than the most- and least-accurate local allometric models. The agreement between TLS–QSM estimates and reference values expressed as CCC is higher (0.96) compared to the most- and least-accurate allometric models (0.76–0.92; Table 5).

For the Indonesian study area, unlike for the Peruvian site, the local allometric models showed lower RMSE and bias than the TLS–QSM for this particular subset of trees. The best local allometric model had a 44% smaller RMSE than the TLS–QSM, was closer to the 1:1 line and had a higher agreement with reference values (CCC = 0.96) than our approach (0.92) (Table 6).

TABLE 4 Accuracies of AGB estimations across sites by the TLS–QSM approach and by pantropical allometric models

Model	RMSE (Mg)	CV RMSE (%)	Bias (%)	Relative error (%)	R^2	Slope	Intercept (Mg)	CCC
TLS–QSM	2.89	28.37	−3.68	−0.33	0.90	1.06	−1.03	0.95
Chave05.m.1.3[a]	3.63	35.60	−15.22	−0.76	0.88	0.77	0.82	0.89
Chave14.eq.7	4.52	44.35	−24.50	−10.49	0.88	0.66	0.94	0.82
Chave05.m.1.6	5.47	53.65	−34.99	−24.91	0.85	0.62	0.33	0.75
Chave14.eq.4[b]	5.60	54.95	−35.67	−24.41	0.85	0.60	0.49	0.73

Sample size = 20 trees.
AGB, above-ground biomass; CCC, concordance correlation coefficient; CV RMSE, coefficient of variation of root mean square error; TLS–QSM, terrestrial laser scanning–quantitative structure models.
[a]Most accurate allometric model.
[b]Least accurate allometric model.

4 | DISCUSSION

4.1 | Consistent and accurate AGB estimation of tropical trees from QSMs

We found that the TLS–QSM approach can provide reliable and accurate AGB estimates for large tropical trees (DBH > 70 cm), outperforming the accuracy of all the pantropical allometric models tested. To the best of our knowledge, this is the first study assessing the accuracy of tropical trees AGB estimates using QSMs from TLS point clouds of trees across different tropical forest regions. A previous study by Disney et al. (2014) presented a proof of concept for the use of TLS–QSM for tree AGB estimation of tropical trees in Gabon, but in their research no tropical trees were harvested, thus the accuracy of its AGB estimates could not be assessed but only compared to the AGB estimates provided by allometric models. Our study showed that AGB estimations by allometric models often are not a reliable indicator of AGB for large tropical trees. This issue was also addressed by Clark and Kellner (2012), Calders, Newnham, et al. (2015) and Ploton et al. (2016). Clark and Kellner (2012) and Calders, Newnham, et al. (2015) both noted that *large trees* are under-represented in calibration

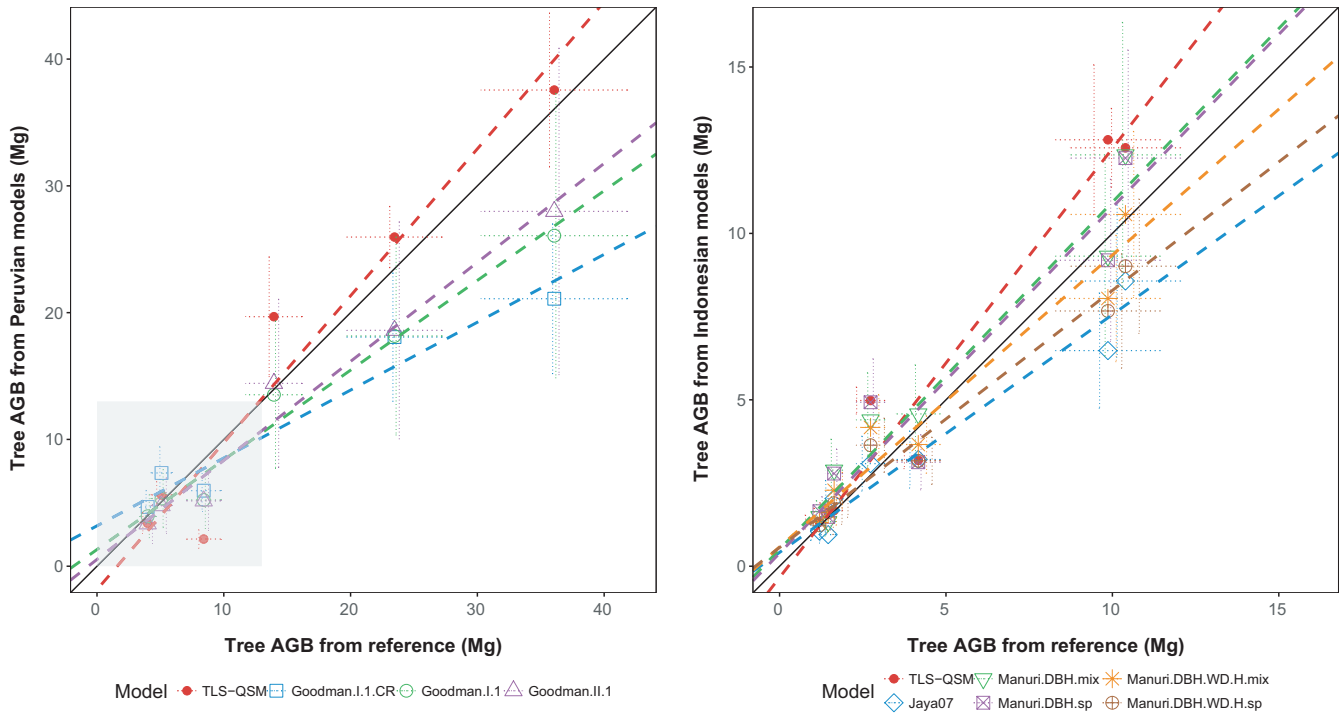

FIGURE 6 Scatterplot of above-ground biomass (AGB) estimates by terrestrial laser scanning–quantitative structure models (TLS–QSM) approach and local allometric models (*y*-axis) against the AGB reference values (*x*-axis) for Peruvian study site (left) and Indonesian study site (right). The 1:1 line is depicted as a black solid line. The dashed lines represents the fitted orthogonal models between AGB estimates by TLS–QSM or local allometric models and AGB reference, with colours corresponding the colour used for the model estimates. Vertical bars show the estimated uncertainty (standard deviation) for each model estimate and horizontal bars show the uncertainty for the reference AGB estimates. Grey box on the left graph shows where the Indonesian values would fit in the Peruvian graph

TABLE 5 Accuracies of AGB estimations for Peruvian trees, by the TLS–QSM and by local allometric models

Model	RMSE (Mg)	CV RMSE (%)	Bias (%)	Relative error (%)	R^2	Slope	Intercept (Mg)	CCC
TLS–QSM	3.68	24.27	3.72	−3.87	0.93	1.16	−1.84	0.96
Goodman.II.1[a]	4.09	26.97	−18.37	−16.87	0.97	0.78	0.54	0.92
Goodman.I.1.CR[b]	7.27	47.98	−26.2	−6.42	0.94	0.54	3.19	0.76

Sample size = 6 trees.
AGB, above-ground biomass; CCC, concordance correlation coefficient; CV RMSE, coefficient of variation of root mean square error; TLS–QSM, terrestrial laser scanning–quantitative structure models.
[a]Most accurate allometric model.
[b]Least accurate allometric model.

TABLE 6 Accuracies of AGB estimations for Indonesian trees, by TLS–QSM approach and by local allometric models

Model	RMSE (Mg)	CV RMSE (%)	Bias (%)	Relative error (%)	R^2	Slope	Intercept (Mg)	CCC
TLS–QSM	1.67	37.13	21.36	19.08	0.96	1.29	−0.34	0.92
Manuri.DBH.WD.H.mix[a]	0.94	20.82	0.63	11.88	0.94	0.88	0.58	0.96
Jaya07[b]	1.52	33.93	−19.33	−12.12	0.95	0.71	0.41	0.89

Sample size = 7 trees.
AGB, above-ground biomass; CCC, concordance correlation coefficient; CV RMSE, coefficient of variation of root mean square error; TLS–QSM, terrestrial laser scanning–quantitative structure models.
[a]Most accurate allometric model.
[b]Least accurate allometric model.

of allometric models, therefore these models may produce large absolute errors for *large trees*, which is supported by our findings. Ploton et al. (2016) identified an increase in the estimation error of pantropical allometric models with the increase of tree mass. Clark and Kellner (2012) also point out that *large trees* inherently span a larger range of AGB values for a given DBH, thus exacerbating this problem of under sampling.

4.1.1 | AGB estimations by TLS–QSM vs. pantropical allometric models

Across the three sites the TLS–QSM method to estimate AGB was more accurate than the most accurate pantropical allometric model evaluated (Chave05 m1.3, in Appendix S5), with an absolute improvement of 7.2% less CV RMSE (Table 4). This accuracy improvement was even more pronounced in terms of bias reduction. Moreover, TLS–QSM showed a higher agreement with reference values (CCC = 0.95) compared to the most accurate pantropical allometric model (CCC = 0.89). Calders, Newnham, et al. (2015) found a comparable trend of higher accuracy for their TLS–QSM method in relation to allometric models for estimating AGB of eucalyptus trees in Australia. The accuracy of the AGB estimates by TLS–QSM in our study was lower than the accuracy reported by Calders, Newnham, et al. (2015), and our agreement (CCC = 0.95) was lower than the agreement found by Calders et al. (CCC = 0.98). This is likely due to the greater structural complexity and vegetation occlusion of the tropical very dense forest in our study areas compared to the open eucalyptus forest studied by Calders, Newnham, et al. (2015). In relation to the updated and widely used pantropical allometric models of Chave et al. (2014), our method achieved an absolute improvement of 16% and 27% lower CV RMSE, which is comparable to the error decrease reported by Calders, Newnham, et al. (2015).

It should be noted that the models accuracies were estimated by comparing each model AGB estimates with AGB reference estimates derived from destructive geometric measurements, rather than with AGB weighted. The uncertainties introduced in measuring stems, buttresses and branches volumes were taken into account, but—as in Kankare et al. (2013) and Berger et al. (2014)—the uncertainty due to the use of Smalian formula for estimating true volume was assumed to be negligible. Furthermore, the uncertainty introduced in the correction factor for small branches volume and in the application of a single species-specific wood density value for each tree instead of discriminating wood density for different woody fractions, both were not measured but taken from literature. Moreover, models uncertainties increasing with tree size indicates heteroscedasticity effects, which should be considered with caution when developing allometric models. This reinforces the need for improved methods for estimating large trees biomass, and for further research with larger datasets to assess the uncertainty on large trees biomass estimation.

4.1.2 | AGB estimations by QSM models vs. local allometric models in Indonesia and Peru

The TLS–QSM method also produced AGB estimates more accurate than the local allometric models for the Peruvian dataset, with a higher agreement (CCC = 0.96) with reference data than the local

allometric models in Peru (CCC = 0.76–0.92). However, several local allometric models outperformed our method for the Indonesian dataset, which trees were predominately smaller than 10 Mg. In this case, several local allometric models had better agreement, ranging from 0.89 to 0.96, while TLS–QSM approach had an agreement of 0.92.

For both cases, at pantropical or regional–local level, there are large implications related to the choice of which allometric model one should use for AGB estimation of tropical trees. While some allometric models presented here performed with similar accuracy than our method for some trees; other allometric models proposed for the same region and by the same authors provided significantly larger errors on the same trees.

4.2 | Reconstructing 3D woody structure of tropical forest trees using QSMs

We showed that the TLS–QSM method can be used to accurately estimate volume from 3D reconstructed structure of large tropical trees from scans in very dense forest with leaf-on conditions. The tree structure reconstructions for these large tropical trees contained larger uncertainty (higher variance on the QSM outcomes) than in previous studies (Calders, Newnham, et al., 2015; Calders et al., 2013; Raumonen et al., 2015) which evaluated smaller trees and were located in more open forest conditions and less occluded trees. For the smallest trees in our study, the 3D reconstruction uncertainty values were closer to those previously reported by Calders, Newnham, et al. (2015).

Consistent with previous QSM studies (Calders, Newnham, et al., 2015; Calders et al., 2013; Disney et al., 2014; Raumonen et al., 2013), we optimized the reconstruction process based on the *PatchDiam* parameter, which was reported to be the most influential parameter (Calders et al., 2013). The main difference compared to Calders, Newnham, et al. (2015) is in the method for judging the optimal reconstruction.

Our sample of tropical trees was characterized by being among the most challenging conditions for a 3D tree reconstruction method because the target trees were among the tallest trees in each plot and having the largest crown size and complexity. The combination of these limiting factors contributes to increased occlusion, in combination with very dense understorey, resulting in under-sampled areas in the tree crowns and larger uncertainties in the QSM reconstructions. For these low-density point cloud areas the QSMs presented some unrealistic branching reconstructions. The low-density point cloud issue was also addressed by Raumonen et al. (2011, 2013). They stated that the reconstruction method was quite sensitive to low point cloud density and therefore, reliability of cylinders reconstructing small branches could be very low. Therefore, we discarded all branches with a diameter <10 cm and applied the expansion factor to account for their volume.

Alternatively, Calders, Burt, et al. (2015) recently proposed an automated method for QSM parameterization. This method optimized the *PatchDiam* value based on the maximum match of QSM cylinders diameter with point cloud circle fitting diameter at four different heights along the main trunk. This approach focuses on comparing the reconstructed main trunk, regardless of the quality of the reconstructed tree crown. However, recent studies (Goodman et al., 2014; Ploton et al., 2016) showed the important contribution of the crown biomass to the total tree biomass for large tropical trees. Similarly, for the trees in our study, the crown contribution to the total tree biomass was 50% on average and even larger for the trees above 10 Mg (60% of the total tree biomass). Therefore, we decided not to implement the method of Calders, Newnham, et al. (2015) for our study.

Future research should focus on developing an automated QSM optimization which optimizes the reconstruction of the entire tree and does not focus on the tree trunk alone. Automated optimization of this sort might enable to improve even further the accuracy of tree volume and AGB estimates of tropical trees from TLS data at large scale without harvesting trees.

5 | CONCLUSIONS

We present an approach to estimate tree wood volume and AGB for large tropical trees that relies on estimates of tree volume based on 3D data from TLS and basic wood density. We show that tree volume estimation of these large tropical trees based on TLS data and QSM provided a CV RMSE of 23.7% in comparison to destructive harvest measurements. Tree AGB estimates derived from TLS–QSM provided better agreement with AGB reference data (28.4% CV RMSE, CCC = 0.95) than AGB estimates based on traditional forest inventory data and pantropical allometric models (33.5%–54.9% CV RMSE, CCC = 0.73–0.82). The allometric models considered in this study showed a systematic underestimation for large trees (DBH > 70 cm), increasing with tree size, contrasting with the largely smaller and non-systematic deviation for the TLS–QSM.

It is important to remark that our results are based on a limited sample size of 29 trees across three ecosystems, while Calders, Newnham, et al. (2015) harvested 65 trees in one ecosystem. Despite this, our results confirmed a recent trend showing that TLS scanning and QSM are able to account for individual tree structure more effectively than allometric models, thus providing tree volume and AGB estimates which are likely to be unbiased by tree size.

This approach can be further used for testing and calibrating new allometric models, since allometric models often have large absolute errors for large trees, which are usually underrepresented in destructive sampling studies. This opens up the opportunity for QSMs derived from TLS measurements to be used in the future for building improved allometric models that might enhance present and past estimates of forest biomass and carbon emissions from tropical forest.

ACKNOWLEDGEMENTS

This research is part of Center for International Forestry Research (CIFOR) Global Comparative Study on REDD^{+}. The funding partners whose support is greatly appreciated include the Norwegian Agency for Development Cooperation (Norad), the Australian Department

of Foreign Affairs and Trade (DFAT), the European Union (EU), the International Climate Initiative (IKI) of the German Federal Ministry for the Environment, Nature Conservation, Building and Nuclear Safety (BMUB) and the CGIAR Research Program on Forests, Trees and Agroforestry (CRP-FTA) with financial support from the donors to the CGIAR Fund. The study received further support from a SilvaCarbon research project (14-IG-11132762-350) on *Measuring forest degradation for REDD+: a synthesis study across five SilvaCarbon countries*. We acknowledge the collaboration of scientist and technicians from CIFOR and associated consultants, and the Guyana Forestry Commission for their support: Louis Verchot, Shijo Joseph, Emilio Perales, John Janovec, I.E. Wiyono, Garik Cruise, Uji Pribadi, Hans Sukhdeo, Walter Huaraca, Filio Farfán, Cesar Vela, Angel Balarezo and Javier Huinga and many local villagers who participate in the field work in Peru, Indonesia and Guyana. M.D. acknowledges support from the UK NERC National Centre for Earth Observation (NCEO). All the authors declare no conflict of interest.

AUTHORS' CONTRIBUTIONS

J.G.T. and A.L. equally co-led the entire study; J.G.T., A.L., H.B., V.A. and M.H. conceived the ideas and designed methodology; J.G.T., A.L., R.G. and S.M. collected the data; J.G.T. and A.L. analysed the data; J.G.T., A.L. and H.B. led the writing of the manuscript. All authors contributed critically to the drafts and gave final approval for publication.

DATA ACCESSIBILITY

The individual trees TLS point cloud, QSM cylinder models, forest inventory and destructive sampling measurement data used for this research can be accessed in the LUCID repository (http://lucid.wur.nl/datasets/terrestrial-lidar-of-tropical-forests). These datasets are owned by the CIFOR and Wageningen University. The datasets are free to download and available for any use as long as the proper reference, as specified in the portal, is applied. For collaborations or questions please contact: jose.tanago@gmail.com, alvaro.lausarmiento@wur.nl or harm.bartholomeus@wur.nl.

ORCID

Jose Gonzalez de Tanago http://orcid.org/0000-0001-5461-8250
Alvaro Lau http://orcid.org/0000-0002-0419-7002
Mathias Disney http://orcid.org/0000-0002-2407-4026

REFERENCES

Bauwens, S., Bartholomeus, H., Calders, K., & Lejeune, P. (2016). Forest inventory with terrestrial LiDAR: A comparison of static and hand-held mobile laser scanning. *Forests*, *7*, 127.

Berger, A., Gschwantner, T., McRoberts, R. E., & Schadauer, K. (2014). Effects of measurement errors on individual tree stem volume estimates for the Austrian National Forest Inventory. *Forest Science*, *60*, 14–24.

Calders, K., Burt, A., Newnham, G., Disney, M., Murphy, S., Raumonen, P., ... Kaasalainen, M. (2015). Reducing uncertainties in above-ground biomass estimates using terrestrial laser scanning. In *Proceedings of Silvilaser* (pp. 197–199). La Grande Motte, France: IRSTEA, IGN.

Calders, K., Newnham, G., Burt, A., Murphy, S., Raumonen, P., Herold, M., ... Kaasalainen, M. (2015). Nondestructive estimates of above-ground biomass using terrestrial laser scanning. *Methods in Ecology and Evolution*, *6*, 198–208.

Calders, K., Newnham, G., Herold, M., Murphy, S., Culvenor, D., Raumonen, P., ... Disney, M. (2013). Estimating above ground biomass from terrestrial laser scanning in Australian Eucalypt Open Forest. In *Proceedings Silvilaser 2013* (pp. 90–97), October 9–11, Beijing, China.

Chave, J., Andalo, C., Brown, S., Cairns, M. A., Chambers, J. Q., Eamus, D., ... Yamakura, T. (2005). Tree allometry and improved estimation of carbon stocks and balance in tropical forests. *Oecologia*, *145*, 87–99.

Chave, J., Condit, R., Salomon, A., Hernandez, A., Lao, S., & Perez, R. (2004). Error propagation and scaling for tropical forest biomass estimates. *Philosophical Transactions: Biological Sciences*, *359*, 409–420.

Chave, J., Coomes, D., Jansen, S., Lewis, S. L., Swenson, N. G., & Zanne, A. E. (2009). Towards a worldwide wood economics spectrum. *Ecology Letters*, *12*, 351–366.

Chave, J., Réjou-Méchain, M., Búrquez, A., Chidumayo, E., Colgan, M. S., Delitti, W. B. C., ... Vieilledent, G. (2014). Improved allometric models to estimate the aboveground biomass of tropical trees. *Global Change Biology*, *20*, 3177–3190.

Clark, D. B., & Kellner, J. R. (2012). Tropical forest biomass estimation and the fallacy of misplaced concreteness. *Journal of Vegetation Science*, *23*, 1191–1196.

Delagrange, S., Jauvin, C., & Rochon, P. (2014). PypeTree: A tool for reconstructing tree perennial tissues from point clouds. *Sensors*, *14*, 4271–4289.

Disney, M., Burt, A., Calders, K., Raumonen, P., Gonzalez de Tanago, J., Sanchez, A. C., ... Lewis, P. (2014). New applications of 3D measurement & modelling for quantifying forest structure & biomass. In *Proceedings of the IC global vegetation monitoring and modeling (GV2M)* (pp. 208–209). Avignon, France.

Gibbs, H. K., Brown, S., Niles, J. O., & Foley, J. A. (2007). Monitoring and estimating tropical forest carbon stocks: Making REDD a reality. *Environmental Research Letters*, *2*, 45023.

Goetz, S. J., & Dubayah, R. (2011). Advances in remote sensing technology and implications for measuring and monitoring forest carbon stocks and change. *Carbon Management*, *2*, 231–244.

Gonzalez de Tanago, J., Lau, A., Bartholomeus, H., Herold, M., Raumonen, P., Avitabile, V. ... Joseph, S. (2016). *Quantification of tropical forest biomass with terrestrial LiDAR and 3D tree quantitative structure modelling*. ESA Living Planet Symposium 2016, Prague: Czech Republic.

Goodman, R. C., Phillips, O. L., & Baker, T. R. (2013). Data from: The importance of crown dimensions to improve tropical tree biomass estimates. *Dryad Digital Repository*, https://doi.org/10.5061/dryad.p281g

Goodman, R. C., Phillips, O. L., & Baker, T. R. (2014). The importance of crown dimensions to improve tropical tree biomass estimates. *Ecological Applications*, *24*, 680–698.

Hackenberg, J., Wassenberg, M., Spiecker, H., & Sun, D. (2015). Non destructive method for biomass prediction combining TLS derived tree volume and wood density. *Forests*, *6*, 1274–1300.

Holopainen, M., Vastaranta, M., & Kankare, V. (2011). Biomass estimation of individual trees using stem and crown diameter TLS measurements. *International Archives of Photogrammetry, Remote Sensing and Spatial Information Sciences*, *VIII*, 29–31.

IPCC. (2006). *2006 IPCC Guidelines for National Greenhouse Gas Inventories* (S. Eggleston, L. Buendia, K. Miwa, T. Ngara, & K. Tanabe Eds.). Hayama, Japan: IGES.

Jaya, A., Siregar, U. J., Daryono, H., & Suhartana, S. (2007). Biomassa hutan rawa gambut tropika pada berbagai kondisi penutupan lahan. *Jurnal Penelitian Hutan dan Konservasi Alam*, *4*, 341–352.

Kankare, V., Vastaranta, M., Holopainen, M., Räty, M., Yu, X., Hyyppä, J., ... Viitala, R. (2013). Retrieval of forest aboveground biomass and stem volume with airborne scanning LiDAR. *Remote Sensing*, *5*, 2257–2274.

Király, G., & Brolly, G. (2007). Tree height estimation methods for terrestrial laser scanning in a forest reserve. *International Archives of Photogrammetry, Remote Sensing and Spatial Information Sciences*, *VI*, 211–215.

Manuri, S., Brack, C., Nugroho, N. P., Hergoualc'h, K., Novita, N., Dotzauer, H., ... Widyasari, E. (2014). Tree biomass equations for tropical peat swamp forest ecosystems in Indonesia. *Forest Ecology and Management*, *334*, 241–253.

Mitchard, E. T. A., Feldpausch, T. R., Brienen, R. J. W., Lopez-Gonzalez, G., Monteagudo, A., Baker, T. R., ... Phillips, O. L. (2014). Markedly divergent estimates of Amazon forest carbon density from ground plots and satellites. *Global Ecology and Biogeography*, *23*, 935–946.

Mitchard, E. T. A., Saatchi, S. S., Baccini, A., Asner, G. P., Goetz, S. J., Harris, N. L., & Brown, S. (2013). Uncertainty in the spatial distribution of tropical forest biomass: A comparison of pan-tropical maps. *Carbon Balance and Management*, *8*, 10.

Molto, Q., Rossi, V., & Blanc, L. (2013). Error propagation in biomass estimation in tropical forests (R. Freckleton, Ed.). *Methods in Ecology and Evolution*, *4*, 175–183.

Muñoz, G., & Grieser, J. (2006). *Climwat 2.0 for CROPWAT*. Rome, Italy: Food and Agriculture Organization (FAO).

Newnham, G. J., Armston, J. D., Calders, K., Disney, M. I., Lovell, J. L., Schaaf, C. B., ... Danson, M. (2015). Terrestrial laser scanning for plot-scale forest measurement. *Current Forestry Reports*, *1*, 239–251.

Nogueira, E. M., Nelson, B. W., & Fearnside, P. M. (2005). Wood density in dense forest in central Amazonia, Brazil. *Forest Ecology and Management*, *208*, 261–286.

Ploton, P., Barbier, N., Momo, S. T., Réjou-Méchain, M., Boyemba Bosela, F., Chuyong, G., ... Pélissier, R. (2016). Closing a gap in tropical forest biomass estimation: Accounting for crown mass variation in pantropical allometries. *Biogeosciences Discussions*, *12*, 19711–19750.

R Core Team. (2013). *R: A language and environment for statistical computing*. Vienna, Austria: The R Foundation for Statistical Computing.

Raumonen, P., Casella, E., Calders, K., Murphy, S., Åkerblom, M., & Kaasalainen, M., (2015). Massive-scale tree modelling from TLS data. *ISPRS Annals of Photogrammetry, Remote Sensing and Spatial Information Sciences*, *II-3/W4*, 189–196.

Raumonen, P., Kaasalainen, M., Åkerblom, M., Kaasalainen, S., Kaartinen, H., Vastaranta, M., ... Lewis, P. (2013). Fast automatic precision tree models from terrestrial laser scanner data. *Remote Sensing*, *5*, 491–520.

Raumonen, P., Kaasalainen, S., Kaasalainen, M., & Kaartinen, H. (2011). Approximation of volume and branch size distribution of trees from laser scanner data. *International Archives of Photogrammetry, Remote Sensing and Spatial Information Sciences*, *VIII*, 1–6.

Segura, M., & Kanninen, M. (2005). Allometric models for tree volume and total aboveground biomass in a tropical humid forest in Costa Rica. *Biotropica*, *37*, 2–8.

Slik, J. W. F., Paoli, G., McGuire, K., Amaral, I., Barroso, J., Bastian, M., ... Zweifel, N. (2013). Large trees drive forest aboveground biomass variation in moist lowland forests across the tropics. *Global Ecology and Biogeography*, *22*, 1261–1271.

Stegen, J. C., Swenson, N. G., Enquist, B. J., White, E. P., Phillips, O. L., Jørgensen, P. M., ... Núñez Vargas, P. (2011). Variation in above-ground forest biomass across broad climatic gradients. *Global Ecology and Biogeography*, *20*, 744–754.

The MathWorks Inc. (2014). *MatLab 2013a and statistics toolbox*. Natick, MA: The MathWorks Inc.

Wilkes, P., Lau, A., Disney, M., Calders, K., Burt, A., Gonzalez de Tanago, J., ... Herold, M. (2016). Data acquisition considerations for terrestrial laser scanning of forest plots (submitted manuscript). *Remote Sensing of Environment*.

Yao, T., Yang, X., Zhao, F., Wang, Z., Zhang, Q., Jupp, D., Strahler, A. (2011). Measuring forest structure and biomass in New England forest stands using Echidna ground-based lidar. *Remote Sensing of Environment*, *115*, 2965–2974.

Zanne, A., Lopez-Gonzalez, G., Coomes, D., Ilic, J., Jansen, S., Lewis, S., ... Chave, J. (2009). *Data from: Towards a worldwide wood economics spectrum*. http://datadryad.org/resource/doi:10.5061/dryad.234

SUPPORTING INFORMATION

Additional Supporting Information may be found online in the supporting information tab for this article.

How to cite this article: Gonzalez de Tanago J, Lau A, Bartholomeus H, et al. Estimation of above-ground biomass of large tropical trees with terrestrial LiDAR. *Methods Ecol Evol*. 2017;00:1–12. https://doi.org/10.1111/2041-210X.12904